Available online at www.sciencedirect.com
ScienceDirect
Computers and Chemical Engineering 32 (2008) 2263–2279
Computers & Chemical Engineering
www.elsevier.com/locate/compchemeng

Selection of an appropriate time integration scheme for the discrete element method (DEM)

H. Kruggel-Emden *, M. Sturm, S. Wirtz, V. Scherer

Department of Energy Plant Technology, Ruhr-Universitaet Bochum, Universitaetsstrasse 150, D-44780 Bochum, Germany

Received 11 June 2007; received in revised form 14 September 2007; accepted 6 November 2007
Available online 17 November 2007

Abstract

With increasing computer power simulation methods addressing discrete problems in a broad range of scientific fields become more and more available. The discrete element method is one of these discontinuous approaches used for modeling granular assemblies. Within this method the dynamics of a system of particles is modeled by tracking the motion of individual particles and their interaction with their adjacencies over time. For the interaction of particles, force models need to be specified. The resulting equations of motion are of coupled ordinary differential configuration, which are usually solved by explicit numerical schemes. In large-scale systems like avalanches, planetary rings, hoppers or chemical reactors vast numbers of particles need to be addressed. Therefore, integration schemes need to be accurate on the one hand, but also numerically efficient on the other hand. This numerical efficiency is characterized by the method's demand for memory and CPU-time. In this paper a number of mostly explicit numerical integration schemes are reviewed and applied to the benchmark problem of a particle impacting a fixed wall as investigated experimentally by Gorham and Kharaz [Gorham, D. A., & Kharaz, A. H. (2000). The measurement of particle rebound characteristics. *Powder Technology*, *112*(3), 193–202]. The accurate modeling which includes the correct integration of the equations of motion is essential. In discrete simulation methods the accuracy of properties on the single particle level directly influence the global properties of the granular assembly like velocity distributions, porosities or flow rates, whereas their correct knowledge is often of key interest in engineering applications. The impact experiment is modeled with simple force displacement approaches which allow an analytical solution of the problem. Aspects discussed are the dependency of the step size on the accuracy of certain collision properties and the related computing time. The effect of a fixed time step is analyzed. Guidelines for the efficient selection of an integration scheme considering the additional computational cost by contact detection and force calculation are presented.

Keywords: Granular dynamics; Integration schemes; Discrete element method; Linear force model; Analytical solution

1. Introduction

The discrete element method as introduced by Cundall and Strack (1979) in 1979 for problems in the field of geosciences is more and more evolving into the numerical method of choice when particle orientated problems need to be addressed. Especially in areas related to the disciplines of chemical engineering or energy technology the discrete element method has become a very popular and powerful simulation tool. To give some examples: Mixing and segregation in drums and on grates was addressed by Van Puyvelde (2006), Yang, Zou, and Yu (2003), Pandey, Song, and Kayihan (2006), Kwapinska, Saage, and Tsotsas (2006), Bertrand, Leclaire, and Levecque (2005), Kruggel-Emden, Simsek, Wirtz, and Scherer (2007), and Peters, Dziugys, Hunsinger, and Krebs (2005), fluidized beds were studied by Limtrakul, Boonsrirat, and Vatanatham (2004), Moon, Kevrekidis, and Sundaresan (2006), Tatemoto, Mawatari, and Noda (2005) and Zhong, Xiong, Yuan, and Zhang (2006) and silo discharge was recently modeled by Arratia, Duong, and Muzzio (2006), Kruggel-Emden, Simsek, Wirtz, and Scherer (2006) and Balevicius, Kacianauskas, and Mroz (2006).

Within discrete element simulations, equations of motion given in the form of coupled ordinary differential equations need to be solved over time. Depending on the size of the system large numbers of particles have to be addressed. As a preliminary action for the calculation of the forces in a typical time step within a discrete element code, the contacts between particles or particles and the surroundings need to be identi-

* Corresponding author.
E-mail address: Kruggel-Emden@leat.rub.de (H. Kruggel-Emden).

0098-1354/$ – see front matter © 2007 Elsevier Ltd. All rights reserved.
doi:10.1016/j.compchemeng.2007.11.002

fied. Although this problem is initially of quadratic order in terms of processing time over the number of particles, several algorithms have been developed reducing the problem to linear/logarithmic and further down to linear order (Allen & Tildesley, 1989; Munjiza & Andrews, 1998; Munjiza, Rougier, & John, 2006; Schinner, 1999). For each existing contact, forces must be calculated which are generally addressed separately in normal and tangential direction. For both groups a large number of models have been developed, varying in their governing mechanism, their computational complexity and their accuracy. Many force models were reviewed in detail based on comparisons with measurements for the normal direction (Kruggel-Emden, Simsek, Rickelt, Wirtz, & Scherer, 2007; Kruggel-Emden, Simsek, Wirtz, et al., 2007; Schäfer, Dippel, & Wolf, 1996; Stevens & Hrenya, 2005) and the tangential direction (Di Renzo & Di Maio, 2004; Kruggel-Emden, Wirtz, & Scherer, in press; Schäfer et al., 1996). With the calculated forces, the equations of motion can be solved numerically and the new positions and velocities for the upcoming time step are available. Within one cycle the integration of the equations of motion only contributes to a fraction of the overall time needed for the necessary calculations. For the solution of the equations of motion several numerical schemes are in use. Methods can be subdivided into three main categories: one-step, multi-step and predictor–corrector methods. Taylor series (Shampine, 1994), Runge-Kutta (Butcher, 1987), central difference (Cundall & Strack, 1979; O'Sullivan & Bray, 2004), position Verlet (Tuckerman, Berne, & Martyna, 1993), and symplectic analytically integrable decomposition schemes (Forest & Ruth, 1990; Omelyan, Mryglod, Folk, & 2002a; Omelyan, Mryglod, & Folk, 2002b) are one-step methods. Multi-step methods are the original Verlet (1967), the Adams–Bashforth (Shampine, 1994), and the Khakimov (2002) schemes. The predictor–corrector algorithms consist of the Adams–Bashforth–Moulton (Engeln-Mullges & Uhlig, 1996) and the Gear's integration schemes (Pöschel & Schwager, 2005).

Although the integration of the equations of motion accounts only for a fraction of the total computational cost in each time step, appropriate integration schemes enable the use of larger time steps and therefore can speed up discrete element simulations significantly.

In the past Zhang and Whiten developed algorithms for the step size control within discrete element simulations (Zhang & Whiten, 2001) and a force summation approach, where the integration of the equations of motion is done a priori to the calculation of the forces which are based on earlier tabulated values (Zhang & Whiten, 1998). Both methods are limited in their applicability. The first approach leads to low efficiencies in dense granular systems, whereas the second approach gets complicated and numerically inefficient, when considered for tangential forces or multi-particle contacts. A different aspect widely discussed in literature is the number of time steps or the step size needed to resolve a collision satisfactory. Recommended values vary strongly and are often stated without consideration of the integration scheme used. Whereas Cundall and Strack (1979) originally recommended a time step of half the size of the duration of a collision of a particle, O'Sullivan and Bray (2004) recommended reducing this value further by a factor of three to five depending on the type of the simulation in combination with the central difference scheme. Dury and Ristow (1997) use a time step of 1/15, Peters et al. (2005) apply a time step of 1/30 and Thompson and Grest (1991) use a time step of 1/50 of the collision time. Langston, Tüzün, and Heyes (1994) recommends a step size of 1/100 of the collision time. A comparison of different numerical integration schemes considering the discrete element method was performed in limited cases only. Rougier, Munjiza, and John (2004) reviewed several numerical explicit schemes applicable for discontinuous modeling. However, they were only applied and tested for modeling a harmonic oscillator, therefore results are transferable to discrete element simulations only with restrictions. Fraige and Langston (2004) performed a study on damping and integration schemes and analyzed just three simple algorithms in the context of a one-dimensional linear spring damper system.

In this paper, a broad range of integration schemes commonly used within discrete element simulations is reviewed and tested for the benchmark problem of a particle impacting a fixed wall as studied experimentally by Gorham and Kharaz (2000). The accurate modeling of such an occurrence with an appropriately selected integration scheme on the single particle level is of great importance. Binary collisions varying in the range from frontal to grazing impacts constitute the most elementary event within granular assemblies. In discrete systems the behavior on the micro scale directly influences properties on the macro scale (Zhu and Yu, 2004, 2005). In case of granular assemblies, these macroscopic properties which may be velocity profiles, flow rates, or porosities are often of key interest in engineering applications. Their accurate estimation is therefore essential.

For the impact problem analyzed here, the governing equations of motion are derived and basic models like linear spring damper approaches are applied to enable an analytical solution for comparison and evaluation of the different integration schemes. Studies on the accuracy of force models (Kruggel-Emden, Simsek, Rickelt, et al., 2007; Kruggel-Emden et al., in press) have revealed that especially the simple linear force models can be of high precision in many contact situations. Furthermore, they are the most commonly used.

2. Governing equations and adjustment of parameters

In the benchmark experimental setup by Gorham and Kharaz (2000) an aluminum oxide sphere impacts an aluminum alloy plate under impact angles varying from 2° to 85°. The particle is released from a constant height corresponding to an impact speed of 3.85 m/s without initial spin. The duration of a collision varies between $t_f = 1.25 \times 10^{-5}$ and 3.4×10^{-5} s. The particle with the mass $m = 0.26$ g and the radius $R = 2.5$ mm impacts the wall under an angle α. A sketch of this situation is given in Fig. 1.

During an impact it can be assumed that the forces in y direction are not influenced by resulting contact forces from rotations in θ and translations in x direction (Dintwa, van Zeebroeck, Tijskens, & Ramon, 2004). In normal direction a linear viscoelastic spring damper system according to Zhang and Whiten (1996) is utilized assuming a contact to be ceased when the nor-

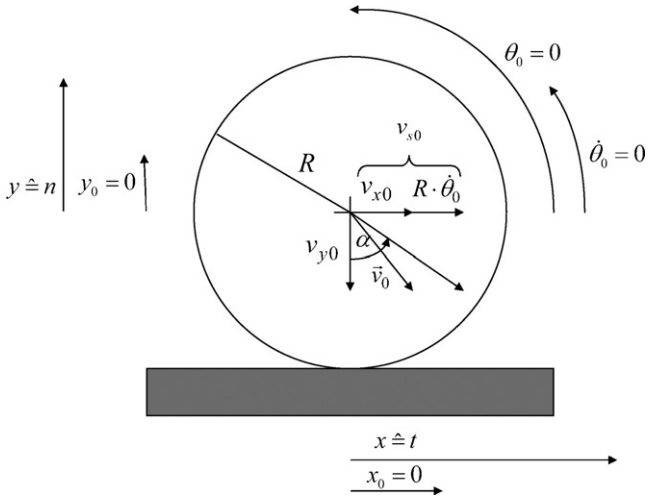

Fig. 1. 2D view of an impact of a spherical particle with a fixed wall at $t = 0$ s.

mal force attains a value of zero. Due to the small timescales the influence of gravitational forces is not considered. In tangential direction a spring limited by the Coulomb condition as proposed by Cundall and Strack (1979) neglecting tangential viscoelasticity is applied, resulting in the following coupled system of ordinary differential equations for the three degrees of freedom:

$$y : m\ddot{y} + \gamma_y \dot{y} + K_y y = 0,$$
$$x : m\ddot{x} + K_x(x + R\theta) = 0, \quad \theta : I\ddot{\theta} + RK_x(x + R\theta) = 0, \quad (1)$$

where K_x, K_y are linear spring stiffnesses and γ_y is a damping coefficient. If the tangential force of the spring exceeds the Coulomb limit $K_x|x + R\theta| > \mu|-\gamma_y\dot{y} - K_y y|$, a different set of differential equations needs to be considered where μ is the dynamic friction coefficient. In this case the force from the tangential linear spring is replaced by the Coulomb formulation as

$$y : m\ddot{y} + \gamma_y \dot{y} + K_y y = 0,$$
$$x : m\ddot{x} + \mu|-\gamma_y\dot{y} - K_y y| = 0,$$
$$\theta : I\ddot{\theta} + R\mu|-\gamma_y\dot{y} - K_y y| = 0. \quad (2)$$

By introduction of the coordinate of the contact point $s = x + R\theta$ and the non-dimensional radius $r = 1 + (mR^2/I) = 7/2$, the sets of equations for the elastic tangential case (1) and for the Coulomb mode (2) simplify significantly.

In the governing Eqs. (1) and (2) the coordinate of the contact point $s = x + R\theta$ during a collision is equivalent to the elongation ξ of the tangential spring in x direction. By limiting the elongation of the spring ξ with $\xi = \text{sign}(\xi) \cdot \mu|-\gamma_y\dot{y} - K_y y|/K_x$ Tsuji, Tanaka, and Ishida (1992) and Di Maio and Di Renzo (2004) motivated by Maw, Barber, and Fawcett (1976) achieved a very good accuracy of the linear model (Kruggel-Emden et al., in press). Therefore, the latter configuration is used here.

For model outlined requires only few properties as the normal stiffness K_y, the normal damping coefficient γ_y, the tangential stiffness K_x and the friction coefficient μ. The linear stiffness K_y and the damping coefficient γ_y can be derived in the context of an extended linear spring damper model as proposed by Kruggel-Emden, Simsek, Rickelt, et al. (2007). In this approach, they are approximated by functions being dependent on the initial normal velocity v_{y0}. To derive these expressions experimental data on the dependency of the coefficient of normal restitution e^n and of the collision time t_f on the initial normal velocity is necessary to adjust the four parameters χ_1, χ_2, χ_3, χ_4 in the two empirical equations $e^n = -v_{yf}/v_{y0} = \chi_1(v_{y0} + v_{00})^{-\chi_2}$ and $t_f = \chi_3(v_{y0})^{-\chi_4}$ with $v_{00} = (\chi_1)^{(1/\chi_2)}$. Gorham and Kharaz (2000) provided detailed data on the coefficient of normal restitution, but no data on the collision times. These are therefore calculated from the elastic Hertz model (Hertz, 1882) which provides a good approximation. The coefficients χ_1–χ_4 are calculated as: $\chi_1 = 0.8377$, $\chi_2 = 0.2121$, $\chi_3 = 0.000017$ and $\chi_4 = 0.1907$. The expressions for K_y and γ_y can then be derived by solving the system of equations formed by the two potential functions stated above and the expression for the coefficient of restitution and the collision time given by

$$e^n = \exp\left(\frac{\delta_y}{\omega_y}\left[\arctan\left[\frac{2\delta_y\omega_y}{\omega_y^2 - \delta_y^2}\right] + \pi\right]\right), \quad (3)$$

$$t_f = \frac{1}{\omega_y}\left[\arctan\left[\frac{2\delta_y\omega_y}{\omega_y^2 - \delta_y^2}\right] + \pi\right] \quad (4)$$

with the two variables $\omega_y = \sqrt{(K_y/m) - (\gamma_y/2m)^2}$ and $\delta_y = -\gamma_y/2m$. The tangential stiffness K_x can be derived as suggested by Schäfer et al. (1996) and Kruggel-Emden et al. (in press) through $K_x = \kappa m\pi^2/(t_f)^2$ where κ is the tangential to normal stiffness ratio and t_f is the contact duration. The stiffness ratio is strongly influencing the performance of the tangential force model. It can be obtained from the mechanical properties of the bodies involved in the collision as $\kappa = ((1 - \nu_i)/G_i + (1 - \nu_j)/G_j)/((1 - 0.5\,\nu_i)/G_i(1 - 0.5\,\nu_j)/G_j)$ with $\nu_i = 0.23$, $\nu_j = 0.345$ the Poisson ratios and $G_i = 154$ GPa, $G_j = 26$ GPa the shear module resulting in $\kappa = 0.8035$. Measurements performed by Gorham and Kharaz (2000) revealed a friction coefficient of $\mu = 0.18$.

3. Applicable numerical schemes

In the following, a summary of common and popular integration schemes is given. Algorithms are tabulated in the three main categories one-step, multi-step, and predictor–corrector algorithms.

3.1. One-step algorithms

The forward Euler, referred to as FE in the following, is based on the first two terms of the Taylor series expansion and results in truncation errors of $O(\Delta t^2)$. The scheme was applied in discrete element simulations by Di Renzo and Di Maio (2004), Melheim (2005), Taguchi (1992a), and Sadd, Tai, and Shukla (1993). The positions and velocities in the upcoming time step $t + \Delta t$ are calculated from the positions and velocities at time step t by

$$r_{t+\Delta t} = r_t + v_t\Delta t, \quad v_{t+\Delta t} = v_t + a_t\Delta t. \quad (5)$$

In case that the accelerations a_t are included into the expression for the positions, the truncation error is reduced to $O(\Delta t^3)$ for the positions, but remains of the order $O(\Delta t^2)$ for the velocities. This scheme is referred to as TY2 and was applied by Taguchi (1992b) and Kruggel-Emden, Simsek, Wirtz, et al. (2007), and Kruggel-Emden et al. (2006); positions and velocities read:

$$r_{t+\Delta t} = r_t + v_t\Delta t + \frac{1}{2}a_t\Delta t^2, \quad v_{t+\Delta t} = v_t + a_t\Delta t. \tag{6}$$

By adding an additional third term, a three term Taylor expansion is generated (TY3). Truncation errors for the positions are of $O(\Delta t^4)$ and of $O(\Delta t^3)$ for the velocities. Positions and velocities in the time step $t+\Delta t$ are calculated from the positions and velocities at time step t as

$$r_{t+\Delta t} = r_t + v_t\Delta t + \frac{1}{2}a_t\Delta t^2 + \frac{1}{6}b_t\Delta t^3,$$
$$v_{t+\Delta t} = v_t + a_t\Delta t + \frac{1}{2}b_t\Delta t^2, \tag{7}$$

where the first time derivative of the acceleration can be calculated as $b_t = \mathrm{d}a_t/\mathrm{d}t$.

The approach of using even higher time derivatives within a Taylor series expansion was practiced by Corliss and Chang (1982) up to as many as thirty terms. We will restrict ourselves to four terms here. The resulting scheme is referred to as TY4 in the following. Truncation errors are reduced by one order in comparison to the TY3 scheme. Positions and velocities unfold as

$$r_{t+\Delta t} = r_t + v_t\Delta t + \frac{1}{2}a_t\Delta t^2 + \frac{1}{6}b_t\Delta t^3 + \frac{1}{2}4c_t\Delta t^4,$$
$$v_{t+\Delta t} = v_t + a_t\Delta t + \frac{1}{2}b_t\Delta t^2 + \frac{1}{6}c_t\Delta t^3, \tag{8}$$

where the higher time derivatives b_t and c_t are calculated as $b_t = \mathrm{d}a_t/\mathrm{d}t$ and $c_t = \mathrm{d}b_t/\mathrm{d}t$.

Sometimes even Runge-Kutta schemes find application within discrete element simulations. While being of high accuracy they are computationally expensive. Melheim (2005) and Chiesa, Melheim, Pedersen, Ingebrigtsen, and Berg (2005) applied an adaptive step size Runge-Kutta–Fehlberg method within the discrete element method and Ovesen, Petersen, and Perram (1996) used a constant step size Runge-Kutta scheme for molecular dynamics. The algorithm considered here, however, is a standard Runge-Kutta scheme having a truncation error of $O(\Delta t^5)$. Positions and velocities are calculated by

$$kr_1 = v_t, \quad kv_1 = a_t; \quad r_2 = r_t + \frac{1}{2}\cdot\Delta t\cdot kr_1,$$
$$v_2 = v_t + \frac{1}{2}\cdot\Delta t\cdot kv_1; \quad kr_2 = v_2, \quad kv_2 = a(r1, v1);$$
$$r_3 = r_t + \frac{1}{2}\cdot\Delta t\cdot kr_2, \quad v_2 = v_t + \frac{1}{2}\cdot\Delta t\cdot kv_2;$$
$$kr_3 = v_2, \quad kv_3 = a(r_3, v_3); \quad r_4 = r_t + \Delta t\cdot kr_3,$$
$$v_4 = v_t + \Delta t\cdot kv_3; \quad kr_4 = v_4, \quad kv_4 = a(r_4, v_4);$$
$$r_{t+\Delta t} = r_t + \Delta t\left(\frac{1}{6}kr_1 + \frac{1}{3}kr_2 + \frac{1}{3}kr_3 + \frac{1}{6}kr_4\right),$$
$$v_{t+\Delta t} = v_t + \Delta t\left(\frac{1}{6}kv_1 + \frac{1}{3}kv_2 + \frac{1}{3}kv_3 + \frac{1}{6}kv_4\right). \tag{9}$$

The central difference scheme, also known as velocity Verlet is a very widely used integration method of second order. In the following it is referred to as CD. It is applied and discussed in the works of Cundall and Strack (1979), Kwapinska et al. (2006), Allen and Tildesley (1989) and O'Sullivan and Bray (2004). The algorithm can be derived as a modification of the method by Verlet (1967). Velocities and positions are calculated for time steps which are $\Delta t/2$ apart. If the central difference scheme is applied to force calculations which are dependent on the position and the velocity, as in discrete element simulations widely used, forces need to be calculated based on velocities and positions being $\Delta t/2$ apart. This was initially proposed by Cundall and Strack (1979) and adopted by several other authors. Velocities in the upcoming time step $t+\Delta t/2$ and positions at $t+\Delta t$ are calculated as

$$v_{t+\Delta t/2} = v_{t-\Delta t/2} + a(r_t, v_{t-\Delta t/2})\Delta t,$$
$$r_{t+\Delta t} = r_t + v_{t+\Delta t/2}\Delta t. \tag{10}$$

By switching velocities, and positions the leap frog or position Verlet (PV) integration scheme is formed, which can be also transformed back into the Verlet (1967) algorithm. For the calculation of viscoelastic forces, velocities and positions from time steps $\Delta t/2$ apart may be used. The algorithm is used in works by Arratia et al. (2006), Allen and Tildesley (1989) and Tuckerman et al. (1993). Positions in the upcoming time step $t+\Delta t/2$ and velocities at $t+\Delta t$ are calculated as

$$r_{t+\Delta t/2} = r_{t-\Delta t/2} + v_t\Delta t,$$
$$v_{t+\Delta t} = v_t + a(r_{t-\Delta t/2}, v_t)\Delta t. \tag{11}$$

Omelyan et al. (2002a,b) have derived several integration schemes for multi-body and molecular dynamics simulations on the basis of extended decomposition schemes. In case of Verlet-like algorithms, only one parameter is involved, which is calculated based on minimizing the influence of truncated terms. The derived algorithm is of second order like the original Verlet algorithm but allows for a higher accuracy. The position Verlet-like algorithm referred to as BABAB, according to the sequence of velocity and position calculations, reads

$$v_1 = v_t + \varepsilon a_t\Delta t, \quad r_1 = r_t + \frac{v_1\Delta t}{2},$$
$$v_2 = v_1 + (1-2\varepsilon)a_1(r_1, v_1)\Delta t,$$
$$r_{t+\Delta t} = r_1 + \frac{v_2\Delta t}{2},$$
$$v_{t+\Delta t} = v_2 + \varepsilon\cdot a_{t+\Delta t}(r_{t+\Delta t}, v_{t+\Delta t})\Delta t, \tag{12}$$

where the parameter ε was derived by Omelyan et al. (2002a) as $\varepsilon = 0.193183328$. For a viscoelastic force model the integration scheme becomes implicit. Therefore, the last equation has to be solved for $v_{t+\Delta t}$ to calculate the velocity at $t+\Delta t$.

A different fourth order scheme was developed by Forest and Ruth (1990) involving seven position and velocity calculations. The scheme is referred to as BABABAB in the following. Velocities and positions in an upcoming time step $t+\Delta t$ are calculated as

$$v_1 = v_t + \left(\varepsilon + \frac{1}{2}\right) a_t \Delta t,\ r_1 = r_t + (2\varepsilon + 1) v_1 \Delta t,$$

$$v_2 = v_1 - \varepsilon\ a_1(r_1, v_1)\Delta t,\ r_2 = r_1 + (-4\varepsilon - 1) v_2 \Delta t,$$

$$v_3 = v_2 - \varepsilon\ a_2(r_2, v_2)\Delta t,\ r_{t+\Delta t} = r_2 + (2\varepsilon + 1) v_3 \Delta t,$$

$$v_{t+\Delta t} = v_3 + \left(\varepsilon + \frac{1}{2}\right) \cdot a_{t+\Delta t}(r_{t+\Delta t}, v_{t+\Delta t})\Delta t \tag{13}$$

with the free parameter ε calculated by Omelyan et al. (2002b) as $\varepsilon = 0.175603596$. The equation for the last calculation of the velocities has to be solved for $v_{t+\Delta t}$ for viscoelastic forces first. The BABABAB scheme becomes implicit in this case.

3.2. Multi-step algorithms

The classical Verlet algorithm (Verlet, 1967), in the text referred to as VE found several applications in discrete element and molecular dynamics simulations (Allen & Tildesley, 1989; Pandey et al., 2006). The algorithm is closely related to the central difference and the position Verlet scheme. Truncation errors become $O(\Delta t^4)$ for the positions and of $O(\Delta t^2)$ for the velocities. However, as velocities are recalculated every time step from the more precise calculated positions their error is not additionally accumulated during the integration. Positions at two successive time steps have to be stored in memory. The positions and velocities in the upcoming time step $t+\Delta t$ read:

$$r_{t+\Delta t} = 2r_t - r_{t-\Delta t} + a_t \Delta t^2, \quad v_{t+\Delta t} = \frac{r_{t+\Delta t} - r_{t-\Delta t}}{2\Delta t}. \tag{14}$$

The Adams–Bashforth integration schemes use previously computed function values for the interpolation of positions and velocities in an upcoming time step $t+\Delta t$. Only one calculation of the acceleration a_t has to be carried out each time step. On the other hand, several values have to be stored in memory depending on the order of the Adams–Bashforth scheme. Adams–Bashforth solvers have been used in the context of discrete element simulations by Takeuchi, Wang, and Rhodes (2004) and Sundaram and Collins (1996). For a second to fifth order Adams–Bashforth scheme, referred to as AB2–AB5, velocities and accelerations from the previous time steps have to be stored to calculate positions and velocities in the upcoming time step $t+\Delta t$:

$$r_{t+\Delta t} = r_t + \Delta t[\delta_1 v_t - \delta_2 v_{t-\Delta t} + \delta_3 v_{t-2\Delta t} - \delta_4 v_{t-3\Delta t} + \delta_5 v_{t-4\Delta t}],$$

$$v_{t+\Delta t} = v_t + \Delta t[\delta_1 a_t - \delta_2 a_{t-\Delta t} + \delta_3 a_{t-2\Delta t} - \delta_4 a_{t-3\Delta t} + \delta_5 a_{t-4\Delta t}]. \tag{15}$$

The integration scheme parameters δ_1–δ_5 are adjusted according to Table 1 for the different order Adams–Bashforth schemes.

Khakimov (2002) developed three third-order algorithms for molecular dynamics applications. The T12 scheme is based on approximating both the first and the second time derivative of the accelerations by central difference approximations of the accelerations. The positions and velocities in an upcoming time step $t+\Delta t$ read:

Table 1
Adams–Bashforth integration scheme parameters δ_1–δ_5

Scheme	δ_1	δ_2	δ_3	δ_4	δ_5
AB2	3/2	1/2	0	0	0
AB3	23/12	16/12	5/12	0	0
AB4	55/24	59/24	37/24	9/24	0
AB5	1901/720	2774/720	2616/720	1274/720	251/720

$$r_{t+\Delta t} = r_t + \frac{v_t \Delta t + 1/12(7a_t - a_{t-\Delta t})\Delta t^2}{1 - 1/12(\mathrm{d}a_t/\mathrm{d}r_t)\Delta t^2},$$

$$v_{t+\Delta t} = v_t + \frac{1}{12}(8a_t + 5a_{t+\Delta t} - a_{t-\Delta t})\Delta t. \tag{16}$$

The D12 scheme is constructed by using the expression for the velocities from the T12 scheme and by approximating the first time derivative of the accelerations through a central difference approximation from the positions. Positions and velocities form out as

$$r_{t+\Delta t} = r_{t-\Delta t} + \frac{r_t - r_{t-\Delta t} + v_t \Delta t + 1/2 a_t \Delta t^2}{1 - 1/12\,(\mathrm{d}a_t/\mathrm{d}r_t)\,\Delta t^2},$$

$$v_{t+\Delta t} = v_t + \frac{1}{12}(8a_t + 5a_{t+\Delta t} - a_{t-\Delta t})\Delta t. \tag{17}$$

The T16 scheme by Khakimov is based on an approximation of the second time derivative of the acceleration by forward difference approximation of the first time derivative of the accelerations. Positions and velocities read:

$$r_{t+\Delta t} = r_t + v_t \Delta t + \frac{a_t \Delta t^2}{2} + \frac{(\mathrm{d}a_t/\mathrm{d}r_t) v_t \Delta t^3}{6},$$

$$v_{t+\Delta t} = \frac{v_t + a_t \Delta t + 1/3(\mathrm{d}a_t/\mathrm{d}r_t) v_t \Delta t^2}{1 - 1/6(\mathrm{d}a_{t+\Delta t}/\mathrm{d}r_{t+\Delta t})\Delta t^2}. \tag{18}$$

3.3. Predictor–corrector algorithms

For a predictor–corrector method, an explicit method (the predictor) extrapolates an initial guess of the solution in an upcoming time step. An implicit method (the corrector) is then used to improve the initial guess. An easy to use predictor–corrector method can be constructed from the explicit Adams–Bashforth method combined with the implicit Adams–Moulton algorithm. The Adams–Bashforth and the Adams–Moulton method are combined so that the Adams–Moulton method is always one order higher than the Adams–Bashforth method (Engeln-Mullges & Uhlig, 1996). Combinations considered are: AB2 + AM3, AB3 + AM4 and AB4 + AM5.

For a combination of the Adams–Bashforth and the Adams–Moulton algorithm, velocities of the previous time steps

Table 2
Adams–Moulton integration scheme parameters η_1–η_5

Scheme	η_1	η_2	η_3	η_4	η_5
AM3	5/12	8/12	1/12	0	0
AM4	9/24	19/24	5/24	1/24	0
AM5	251/720	646/720	264/720	106/720	19/720

Table 3
Gear's scheme parameters ϑ_1–ϑ_5

Scheme	ϑ_1	ϑ_2	ϑ_3	ϑ_4	ϑ_5
GPC3	1/12	5/12	1	1	0
GPC4	19/240	3/8	1	3/2	1

have to be kept in memory. Positions and velocities in the prediction step are calculated according to Eq. (15). The integration scheme parameters δ_1–δ_5 are calculated according to Table 1. The final positions and velocities according to the Adams–Moulton formula at time step $t+\Delta t$ are obtained from

$$r_{t+\Delta t}=r_t+\Delta t[\eta_1 v_{t+\Delta t,p}+\eta_2 v_t-\eta_3 v_{t-\Delta t}+\eta_4 v_{t-2\Delta t}-\eta_5 v_{t-3\Delta t}],$$
$$v_{t+\Delta t}=v_t+\Delta t[\eta_1 a_{t+\Delta t,p}+\eta_2 a_t-\eta_3 a_{t-\Delta t}+\eta_4 a_{t-2\Delta t}-\eta_5 a_{t-3\Delta t}], \quad (19)$$

where the parameters η_1–η_5 are calculated according to Table 2.

A different class of predictor–corrector schemes very commonly used for molecular dynamics and discrete element applications are Gear's schemes (Allen & Tildesley, 1989; Balevicius, Kacianauskas, et al., 2006; Peters et al., 2005; Thompson and Grest, 1991). They are based on three stages, whereas in addition to the predictor and corrector step known from the Adams-method an evaluation step is added. Schemes considered here are the third order Gear's method (GPC3) and the fourth order Gear's method (GPC4).

In the prediction step positions and their higher derivatives are calculated based on Taylor series expansions as

$$r_{t+\Delta t,p} = r_t + v_t\Delta t + \frac{1}{2}a_t\Delta t^2 + \frac{1}{6}b_t\Delta t^3 + \frac{1}{24}c_t\Delta t^4,$$
$$v_{t+\Delta t,p} = v_t + a_t\Delta t + \frac{1}{2}b_t\Delta t^2 + \frac{1}{6}c_t\Delta t^3,$$
$$a_{t+\Delta t,p} = a_t + b_t\Delta t + \frac{1}{2}c_t\Delta t^2,$$
$$b_{t+\Delta t,p} = b_t + c_t\Delta t,\ c_{t+\Delta t,p} = c_t \quad (20)$$

with the first and second derivative of the accelerations calculated as $b_t = \mathrm{d}a_t/\mathrm{d}t$, $c_t = 0$ for the GPC3 and $b_t = \mathrm{d}a_t/\mathrm{d}t$, $c_t = \mathrm{d}b_t/\mathrm{d}t$ for the GPC4 scheme.

In the evaluation step the difference in the accelerations calculated based on the acceleration $a_{t+\Delta t,p}$ and the acceleration $a_{t+\Delta t}$ calculated from positions $r_{t+\Delta t,p}$ and velocities $v_{t+\Delta t,p}$ is obtained by

$$\Delta a = a_{t+\Delta t} - a_{t+\Delta t,p}. \quad (21)$$

In the following, correction step positions and their higher derivatives are calculated based on their values from the previous time step and the obtained difference in acceleration as

$$r_{t+\Delta t} = r_{t+\Delta t,p} + \vartheta_1\Delta a\Delta t^2,\ v_{t+\Delta t} = v_{t+\Delta t,p} + \vartheta_2\Delta a\Delta t,$$
$$a_{t+\Delta t} = a_{t+\Delta t,p} + \vartheta_3\Delta a,\ b_{t+\Delta t} = b_{t+\Delta t,p} + \vartheta_4\frac{\Delta a}{\Delta t},$$
$$c_{t+\Delta t} = c_{t+\Delta t,p} + \vartheta_5\frac{\Delta a}{\Delta t^2}, \quad (22)$$

where the parameters ϑ_1–ϑ_5 are calculated according to Table 3.

4. Comparison of the algorithms

In the following, the previously introduced numerical integration schemes are compared in terms of their accuracies achieved for a number of characteristic collision properties and later for their CPU-requirements. Collision properties studied are the normal coefficient of restitution $e^{\mathrm{n}} = -v_{\mathrm{yf}}/v_{y0}$ and the tangential coefficient of restitution $e^{\mathrm{t}} = v_{x\mathrm{f}}/v_{x0}$ which are given as the ratio of the final to the initial velocity in both normal and tangential direction. Additionally, the rebound angle $\beta = 180/\pi\arctan(-(v_{x0}\cdot e^{\mathrm{t}})/(v_{y0}\cdot e^{\mathrm{n}}))$ which is dependent on the normal and tangential coefficients of restitution, and the final rotational speed $\dot{\theta}_{\mathrm{f}} = \omega_{\mathrm{f}}$ which can be directly obtained from the solution of the ordinary differential equations are considered. Deviations of the integration algorithms are calculated as average relative deviations between an exact analytical solution and the numerical solution from the schemes as

$$\mathrm{ARD}(\phi) = \frac{1}{N}\sum_{n=1}^{N} 100 \times \left|\frac{\phi_{\mathrm{num},n} - \phi_{\mathrm{analy},n}}{\phi_{\mathrm{analy},n}}\right|, \quad (23)$$

where $N = 100$ is the number of different impact angles considered for the calculation of the average relative deviation $\mathrm{ARD}(\phi)$. The analytical solution of the impact problem is derived in detail in Kruggel-Emden, Wirtz, and Scherer (2007). Only a brief overview shall be given here.

For the analytical solution the y-direction in the sets of Eqs. (1) and (2) is always independent of the direction in $s = x + R\theta$. The solution for the displacement and the velocity can therefore be derived as

$$y(t) = \frac{v_{y0}}{\omega_y}\exp(\delta_y t)\sin(\omega_y t), \quad (24)$$

$$\dot{y}(t) = \frac{v_{y0}}{\omega_y}\delta_y\exp(\delta_y t)\sin(\omega_y t) + v_{y0}\exp(\delta_y t)\cos(\omega_y t). \quad (25)$$

The solution for the elastic case of the contact point s and the center of mass x in the tangential direction can be obtained as

$$s(t) = \left[s_0\cos(\omega_s t_0) - \frac{v_{s0}}{\omega_s}\sin(\omega_s t_0)\right]\cos(\omega_s t) + \left[s_0\sin(\omega_s t_0) + \frac{v_{s0}}{\omega_s}\cos(\omega_s t_0)\right]\sin(\omega_s t), \quad (26)$$

$$\dot{s}(t) = [-s_0\omega_s\cos(\omega_s t_0) + v_{s0}\sin(\omega_s t_0)]\sin(\omega_s t) + [s_0\omega_s\sin(\omega_s t_0) + v_{s0}\cos(\omega_s t_0)]\cos(\omega_s t), \quad (27)$$

Table 4
Name, abbreviation and reference to the equations of all introduced integration schemes

Scheme	Abbreviation	Reference to equation
Forward Euler	FE	(5)
2nd order Taylor expansion	TY2	(6)
3rd order Taylor expansion	TY3	(7)
4th order Taylor expansion	TY4	(8)
Runge-Kutta	RK	(9)
Central difference	CD	(10)
Position Verlet	PV	(11)
Verlet-like BABAB	BABAB	(12)
Verlet-like BABABAB	BABABAB	(13)
Verlet	VE	(14)
2nd–5th order Adams–Bashforth	AB2–AB5	(15)
Khakimov D12	D12	(17)
Khakimov T12	T12	(16)
Khakimov T16	T16	(18)
Adams–Bashforth and Adams–Moulton predictor–corrector	AB2 + AM3, AB3 + AM4, AB4 + AM5	(15) and (19)
3rd and 4th order Gear's	GPC3, GPC4	(20)–(22)

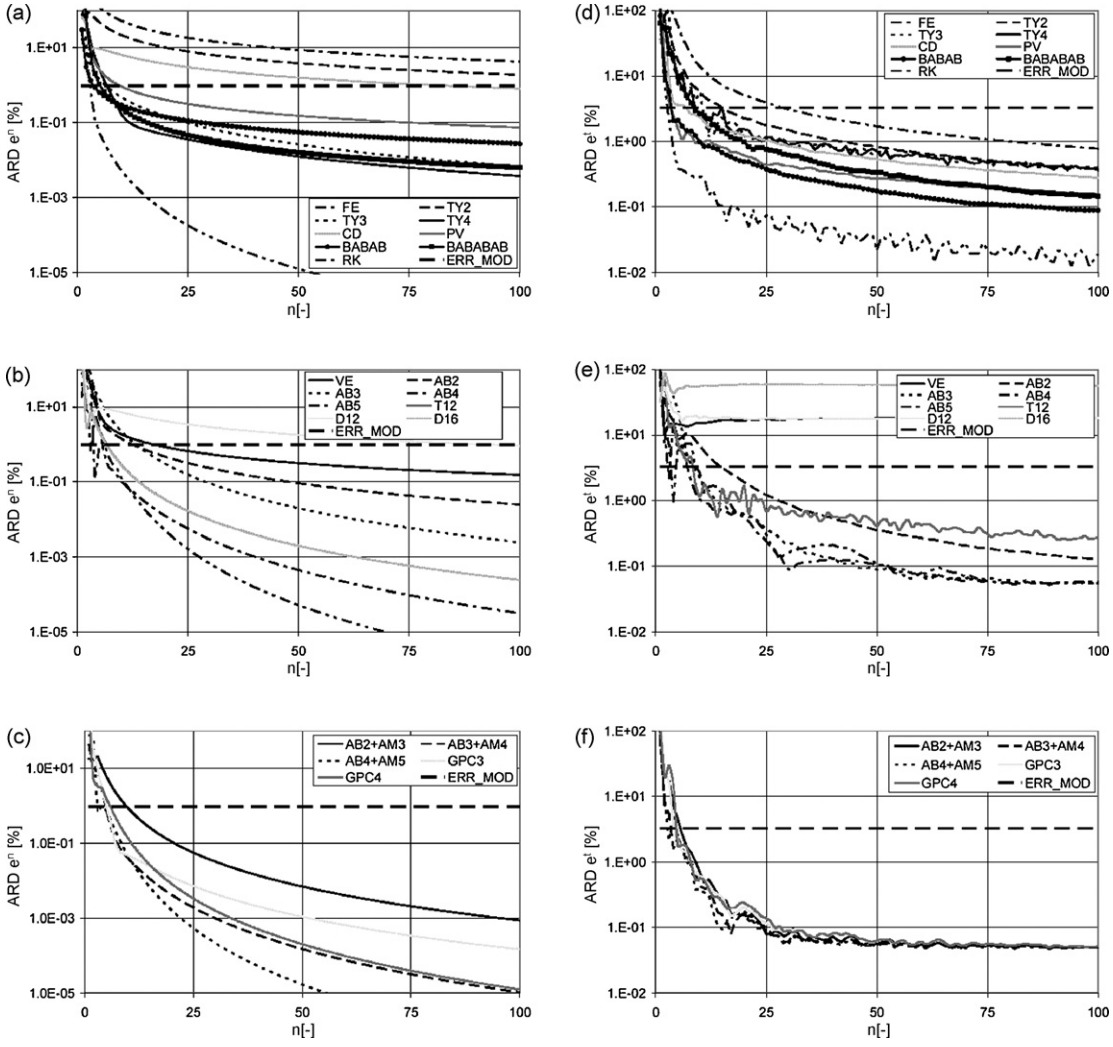

Fig. 2. Average deviation of the normal coefficient of restitution e^n (a–c) and the tangential coefficient of restitution e^t (d–f) between the exact analytical and a numerical solution with varying integration steps for the impact problem by Gorham and Kharaz (2000) for a set of integration schemes.

$$x(t) = x_0 + C_3(\sin(\omega_s t) - \sin(\omega_s t_0)) + C_4(\cos(\omega_s t) - \cos(\omega_s t_0)) + (t - t_0)[v_{x0} - C_3\omega_s \cos(\omega_s t_0) + C_4\omega_s \sin(\omega_s t_0)], \quad (28)$$

$$\dot{x}(t) = v_{x0} + C_3\omega_s[\cos(\omega_s t) - \cos(\omega_s t_0)] + C_4\omega_s[-\sin(\omega_s t) + \sin(\omega_s t_0)], \quad (29)$$

where $\omega_s = \sqrt{rK_x/m}$ and the two coefficients C_3 and C_4 are derived as

$$C_3 = \frac{s_0 \sin(\omega_s t_0) + v_{s0}/\omega_s \cos(\omega_s t_0)}{r}, \quad (30)$$

$$C_4 = \frac{s_0 \cos(\omega_s t_0) - v_{s0}/\omega_s \sin(\omega_s t_0)}{r}. \quad (31)$$

The displacements and velocities in s- and x-direction in Coulomb mode are derivable as

$$s(t) = A(\exp(\delta_y t)\sin(\omega_y t) - \exp(\delta_y t_0)\sin(\omega_y t_0)) + B(\exp(\delta_y t)\cos(\omega_y t) - \exp(\delta_y t_0)\cos(\omega_y t_0)) + (t - t_0)[v_{s0} - A\omega_y \exp(\delta_y t_0)\cos(\omega_y t_0) - B\delta_y \exp(\delta_y t_0)\cos(\omega_y t_0) - A\delta_y \exp(\delta_y t_0)\sin(\omega_y t_0) + B\omega_y \exp(\delta_y t_0)\sin(\omega_y t_0)] + s_0, \quad (32)$$

$$\dot{s}(t) = v_{s0} + (A\omega_y + B\delta_y)[\exp(\delta_y t)\cos(\omega_y t) - \exp(\delta_y t_0)\cos(\omega_y t_0)] + (A\delta_y - B\omega_y)[\exp(\delta_y t)\sin(\omega_y t) - \exp(\delta_y t_0)\sin(\omega_y t_0)], \quad (33)$$

$$x(t) = C(\exp(\delta_y t)\sin(\omega_y t) - \exp(\delta_y t_0)\sin(\omega_y t_0)) + D(\exp(\delta_y t)\cos(\omega_y t) - \exp(\delta_y t_0)\cos(\omega_y t_0)) + (t - t_0)[v_{x0} - C\omega_y \exp(\delta_y t_0)\cos(\omega_y t_0) - D\delta_y \exp(\delta_y t_0)\cos(\omega_y t_0) - C\delta_y \exp(\delta_y t_0)\sin(\omega_y t_0) + C\omega_y \exp(\delta_y t_0)\sin(\omega_y t_0)] + x_0, \quad (34)$$

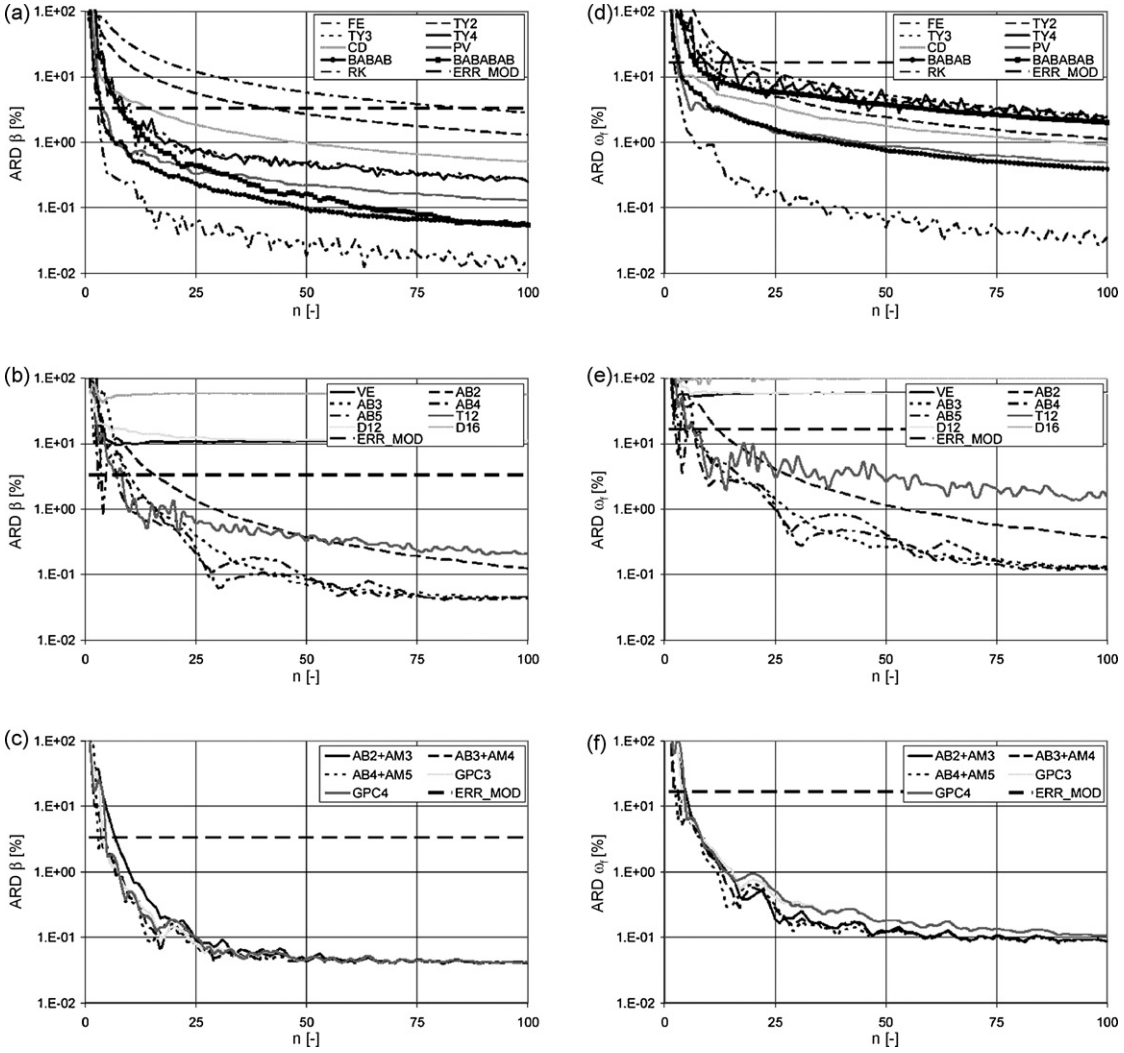

Fig. 3. Average deviation of the rebound angle β (a–c) and the final rotational speed ω_f (d–f) between the exact analytical and a numerical solution with varying integration steps for the impact problem by Gorham and Kharaz (2000) for a set of integration schemes.

$$\dot{x}(t) = v_{x0} + (C\omega_y + D\delta_y)[\exp(\delta_y t)\cos(\omega_y t) - \exp(\delta_y t_0)\cos(\omega_y t_0)] + (C\delta_y - D\omega_y)[\exp(\delta_y t)\sin(\omega_y t) - \exp(\delta_y t_0)\sin(\omega_y t_0)]. \quad (35)$$

The constants A and B in the Eqs. (32) and (33) are derived as $A = |C_1|$, $B = |C_2|$. The constants C and D in Eqs. (34) and (35) are given with $C = |C_1|/r$, $D = |C_2|/r$, where C_1 and C_2 are calculated as

$$C_1 = \frac{r\mu v_{y0}(K_y\delta_y^2 + \gamma_y\delta_y^3 - K_y\omega_y^2 + \gamma_y\delta_y\omega_y^2)}{m\omega_y(2\delta_y^2\omega_y^2 + \delta_y^4 + \omega_y^4)}, \quad (36)$$

$$C_2 = -\frac{r\mu v_{y0}(2K_y\delta_y + \gamma_y\delta_y^2 + \gamma_y\omega_y^2)}{m(2\delta_y^2\omega_y^2 + \delta_y^4 + \omega_y^4)}. \quad (37)$$

With the framework of equations introduced in Section 4, a detailed analytical explicit solution of all relevant collision properties can be derived for both normal and tangential direction. The collision is characterized by three different collision modes depending on the impact angle $\alpha = \arctan(v_{s0}/v_{y0}) = \arctan((v_{x0} + R \cdot \dot{\theta}_0)/v_{y0})$. The points in time $t_1 - t_3$, where the collision mode changes, are derivable from the intersections of the different tangential forces. For details see Kruggel-Emden, Wirtz, and Scherer (2007).

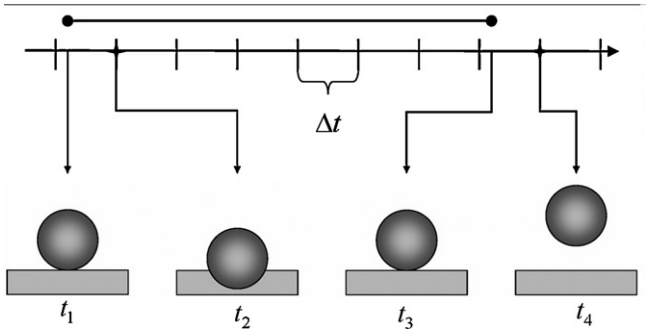

Fig. 4. Error made for the detection of a particle–wall collision with a fixed time step.

4.1. Integration accuracy

In the following, the accuracy of the collision properties resolved by a selected integration scheme is presented. For clar-

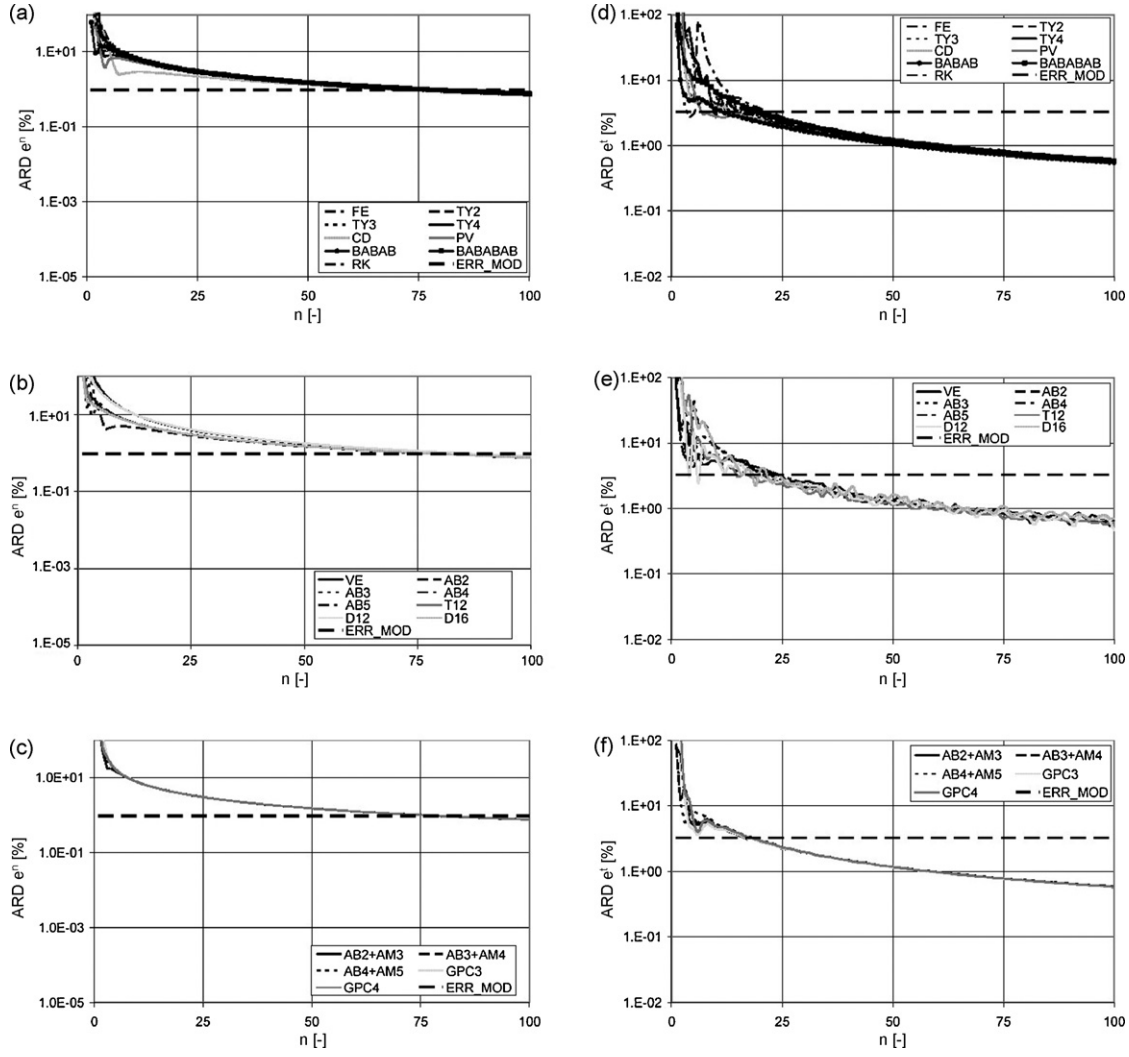

Fig. 5. Average maximal deviation related to a fixed time grid for the normal coefficient of restitution e^n (a–c) and the tangential coefficient of restitution e^t (d–f) for an impact problem as studied by Gorham and Kharaz (2000) for a set of integration schemes.

ity all integration schemes introduced in the previous sections are summarized in Table 4 with their name, their abbreviation and the reference to the corresponding equation.

The average relative deviation of a specific scheme is given as a function of the number of time steps n used, which is a characteristic value usually stated for any simulation performed. In addition to the integration error, the model error, also calculated as average relative deviation between experimental and exact analytical solution, is given in the plots presented. Therefore it is possible to evaluate a certain integration scheme on the background of the accuracy achieved by the model applied.

Fig. 2 shows the deviation of the normal and tangential coefficient of restitution e^{n} and e^{t} for single, multi-step, and predictor–corrector schemes. The model errors of 1% of the applied extended linear spring damper model (Kruggel-Emden, Simsek, Rickelt, et al., 2007) for the coefficient of normal restitution and of 4% for the combination of a linear spring with the Coulomb condition (Kruggel-Emden et al., in press) for the coefficient of tangential restitution are shown as dotted lines.

Integration errors for the normal coefficient of restitution decline continuously with increasing step size. For the normal coefficient of restitution, the forward Euler (FE) and the second order Taylor expansion (TY2) do not manage to get below the model error over the whole range of selected step size numbers ranging from 0 to 100. The central difference scheme (CD) gets below this margin at around 75 steps, the position Verlet (PV) at 10 steps. The improved Verlet scheme (BABAB) and the Taylor expansion of third and fourth order (TY3, TY4) achieve an integration error less than the model error for step numbers larger than 8. Of remarkable accuracy are the (BABABAB) scheme (Forest & Ruth, 1990) and the Runge-Kutta scheme getting below the model error already after 6 steps. Results for the multi-step methods plotted in Fig. 2(b) show the Khakimov scheme (D12) to be of low exactness, achieving the model accuracy for time step numbers of about 95. The Verlet algorithm attains comparable accuracy as the TY3 scheme. The Adams–Bashforth schemes vary in accuracy depending on their order. The second order scheme performs as good as the TY3 scheme, whereas the fifth order Adams–Bashforth scheme achieves the accuracy

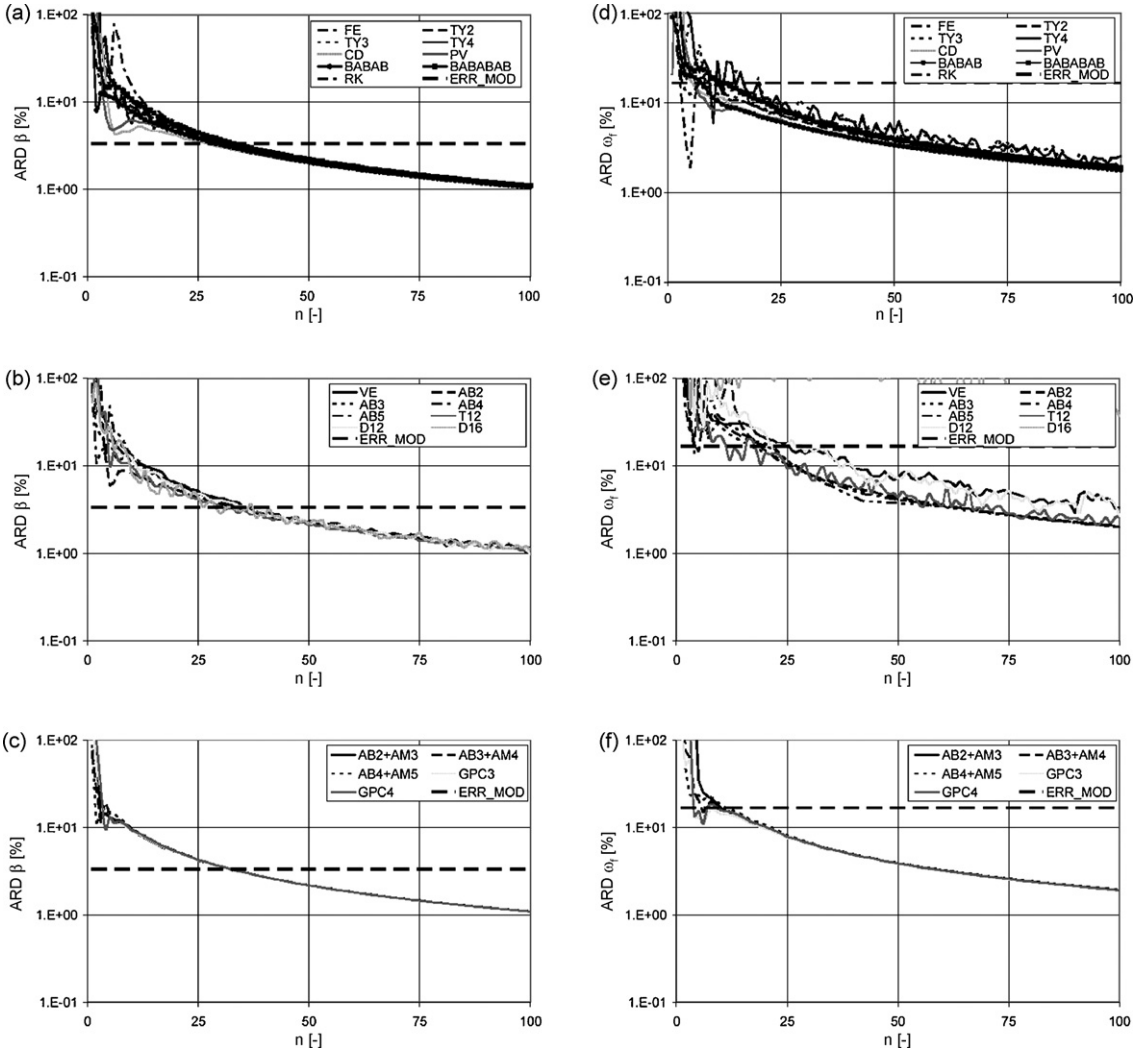

Fig. 6. Average maximal deviation related to a fixed time grid for the rebound angle β (a–c) and the final rotational speed ω_f (d–f) for an impact problem as studied by Gorham and Kharaz (2000) for a set of integration schemes.

of the Runge-Kutta method. The Khakimov schemes T16 and T12 are of high precision being as accurate as a fourth order Adams–Bashforth scheme. The predictor–corrector methods as plotted in Fig. 2(c) always manage to improve accuracy in comparison to the related multi-step methods.

The average relative deviation as calculated for the tangential coefficient of restitution is similar to the accuracy calculated for the normal coefficient of restitution decreasing with increasing numbers of integration steps. However, due to the discontinuous nature of the differential equations in this case, the results for the deviation show slight oscillations for some of the integration schemes considered here. With increasing number of integration steps the reduction of the deviation for the tangential coefficient of restitution is of lower magnitude compared to the increase in accuracy possible for the coefficient of normal restitution. In general, the differences in deviation observed for schemes of one particular class of methods is highest for the single step methods and declines for multi-step and nearly vanishes for predictor–corrector algorithms. From the single step methods the position Verlet (PV) and the (BABAB) scheme reveal a low error. On the other hand, some of the more complex multi-step methods fail. Especially the Verlet (VE) and the Khakimov D12 and T16 schemes result in integration errors larger than 10%. A certain integration scheme has always been applied for the integration of the complete set of differential equations describing the collision. The elongation of the tangential spring ξ, which is adjusted in case that the Coulomb force is exceeded, makes it impossible to use previous positions for the extrapolation of the positions in an upcoming time step as done in the Verlet algorithm. The two Khakimov D12 and T16 schemes encounter difficulties with the integration of certain differential equations. The first faces problems for the integration of the particle's rotation and the second fails for both the calculation of the particle's rotation and the integration of the elongation of the spring. In the two cases the approximations of the higher time derivatives of the accelerations lead to problems. In general most integration schemes result in integration errors of the order of the model accuracy for integration step numbers larger than 20.

In Fig. 3 results for the accuracy of the rebound angle β and the final rotational speed ω_f are plotted. In general, results turn out similar to those for the coefficient of tangential restitution. The accuracy of both properties increases with inclining number of integration steps. For the rebound angle β, forward Euler and Taylor expansions of second order are of comparable low accuracy. Of the simple integration schemes the Taylor method of third order, the position Verlet (PV), and the (BABAB) scheme achieves good accuracy. In general the improvement in accuracy by applying a complex multi-step or a predictor–corrector method is low. For integration step numbers larger than 15, the model accuracy is obtained. In case of the rotational speed ω_f step size numbers larger than 20 insure to match the accuracy of the model. As already observed for the tangential coefficient of restitution, the Verlet (VE), Khakimov D12, and the Khakimov T16 scheme fail to reproduce both collision properties in an adequate manner.

4.2. Time grid accuracy

For the accurate modeling of a collision within a discrete element simulation not only the number of steps is relevant from the point of view of imposing the level of detail in which the collision may be resolved, but also the fixed time step itself introduces additional errors. The beginning and the end of a collision may only be detected at fixed points of time determined through the step size used. The phenomenon is outlined in Fig. 4. A particle is impacting a fixed boundary at a time t_1. Due to the fixed time grid the collision is in the first instance observed at the following time step at t_2. At this point of time an overlap between particle and fixed boundary has already developed and the particle should have lost some of its kinetic energy, however,

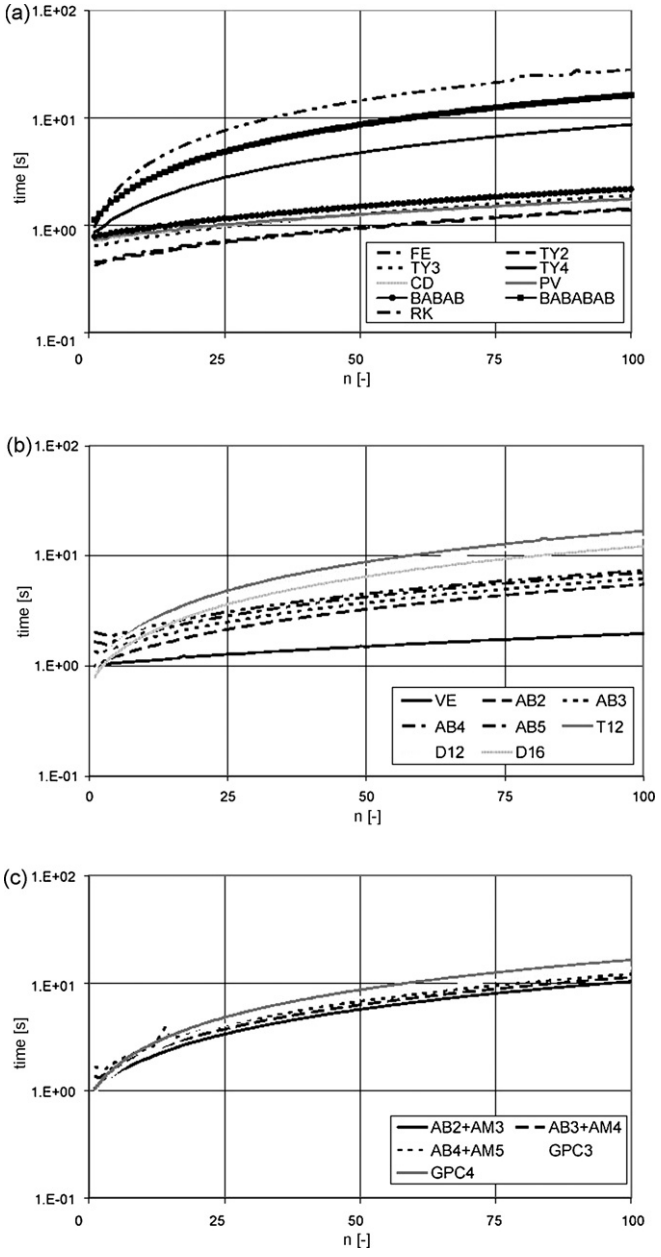

Fig. 7. (a–c) CPU requirement for the solution of the impact problem by Gorham and Kharaz (2000). The impact angle is varied with 0.01°.

instead it has performed a uniform motion until here. With a time grid detailed enough it is possible to detect the collision terminated at t_3. But, due to the low resolution of the step size applied, the end of the contact is detected not until t_4, whereas here the particle is already fully separated from the boundary. The time step is often chosen as a fraction of the real collision time. Therefore, the maximum error is obtained for a collision where the time of contact t_1 is delayed by a minimal time fraction with regard to one of the fixed points of time determined by the constant time step.

The error described is best disclosed for the studied collision properties and the considered integration schemes by analyzing the deviation of the schemes in the two cases of a collision initially occurring and detected at t_1 and the case where the occurrence of a collision is slightly delayed relative to the fixed time grid. Results for the coefficient of normal restitution e^n and the tangential coefficient of restitution e^t are presented in Fig. 5. For the normal coefficient of restitution all integration schemes allow an error of less than the size of the model error for step size numbers larger than 75. For the tangential coefficient of restitution e^t step sizes of above 20 allow for a deviation between fixed time grid and adjustable time grid below the error of the model.

The results for the discrepancy between rebound angle β and the final rotational speed ω_f calculated from the fixed and the adjustable grid are outlined in Fig. 6. For the rebound angle the effect of a fixed time grid is negligible for time step numbers larger than 30. For the final rotational speed ω_f a choice of the step size number larger than 20 allows for staying below the limit of the model error for most of the integration schemes.

4.3. CPU-requirements

Especially in discrete element simulations, the CPU-requirement is the dominating bottleneck for large-scale simulations. Therefore, algorithms are analyzed with respect to their CPU-requirement in the following. To get a measurable result, several impact experiments are performed and the processing time is measured. The results presented here are obtained

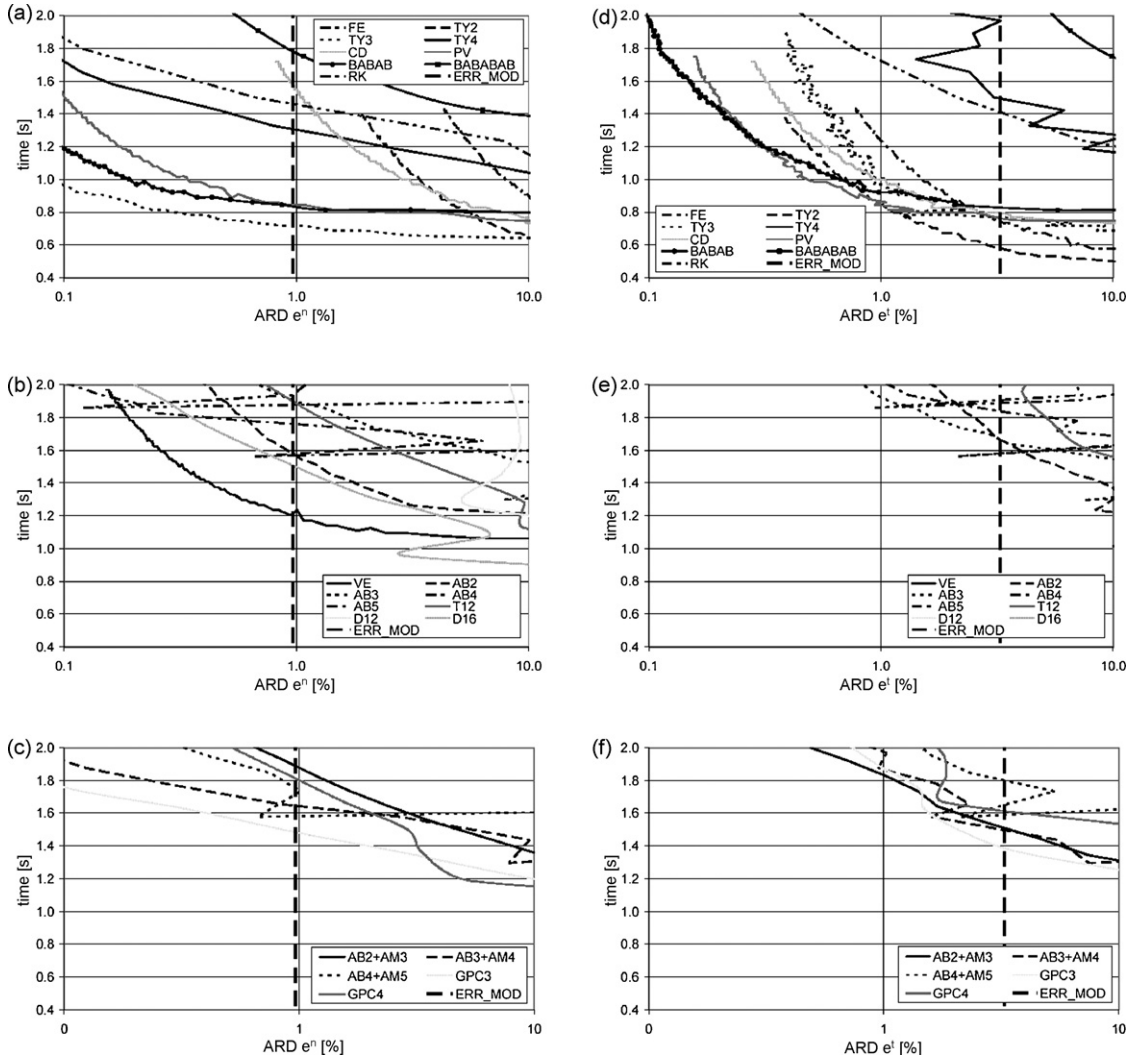

Fig. 8. CPU requirement over the average deviation of the normal coefficient of restitution e^n (a–c) and tangential coefficient of restitution e^t (d–f) between the exact analytical and a numerical solution with varying integration steps for the impact problem by Gorham and Kharaz (2000) for a set of integration schemes.

for varying impact angles between 0 and 90° with an increment of 0.01° on an AMD Athlon XP 2600+ with 1.92 GHz and 512 MB RAM using MATLAB.

Fig. 7 shows the CPU-requirement in the form of the computing time over the number of integration steps applied. A low demand in computing time have the forward Euler (FE), the central difference (CD), the position Verlet (PV), the Verlet (VE), the improved Verlet (BABAB) and the Taylor series expansions of second and third order (TY2, TY3). The Adams–Bashforth solver (AB2, AB3, AB4, AB5) and the Taylor expansion of fourth order (TY4) show a moderate demand for computing time, whereas all other schemes like the Khakimov schemes, the Forest Ruth (BABABAB) algorithm, the predictor–corrector and the Runge-Kutta scheme are highly time consuming.

4.4. Computational efficiency

In order to gain insight into the efficiency of a certain integration scheme the deviation of each collision property has to be plotted over the computing time. With an accuracy level selected from these diagrams, it is possible by Figs. 2 and 3 to identify the related integration step number. Based on Figs. 5 and 6 it is possible to quantify the additional time grid error.

Fig. 8 shows results for the normal and tangential coefficient of restitution e^n and e^t. The model error is indicated as dotted line in the figures. It is feasible to use integration schemes which are at least of lower error than the error introduced by the model. For the normal coefficient of restitution, which suffers from a model error of 1%, it is reasonable to select a method which achieves an integration error of at least 0.5%. In this error range the Taylor expansion series of third order (TY3) is followed by the improved Verlet type algorithm (BABAB) in their efficiency. For the Taylor expansion series of third order (TY3) a deviation of 0.5% corresponds to an integration step number of 18. The error additionally introduced by a fixed time grid is of the size of 4% and therefore considerable higher than the error introduced through the integration method. For the tangential coefficient of restitution, which has a model error of 4%, an integration scheme should be at least of an error lower than 2%. For such an intended deviation, the Taylor expansion series of second order (TY2) shows the best performance. A deviation of 2% corresponds to a step size number of 22 which results in an additional grid error

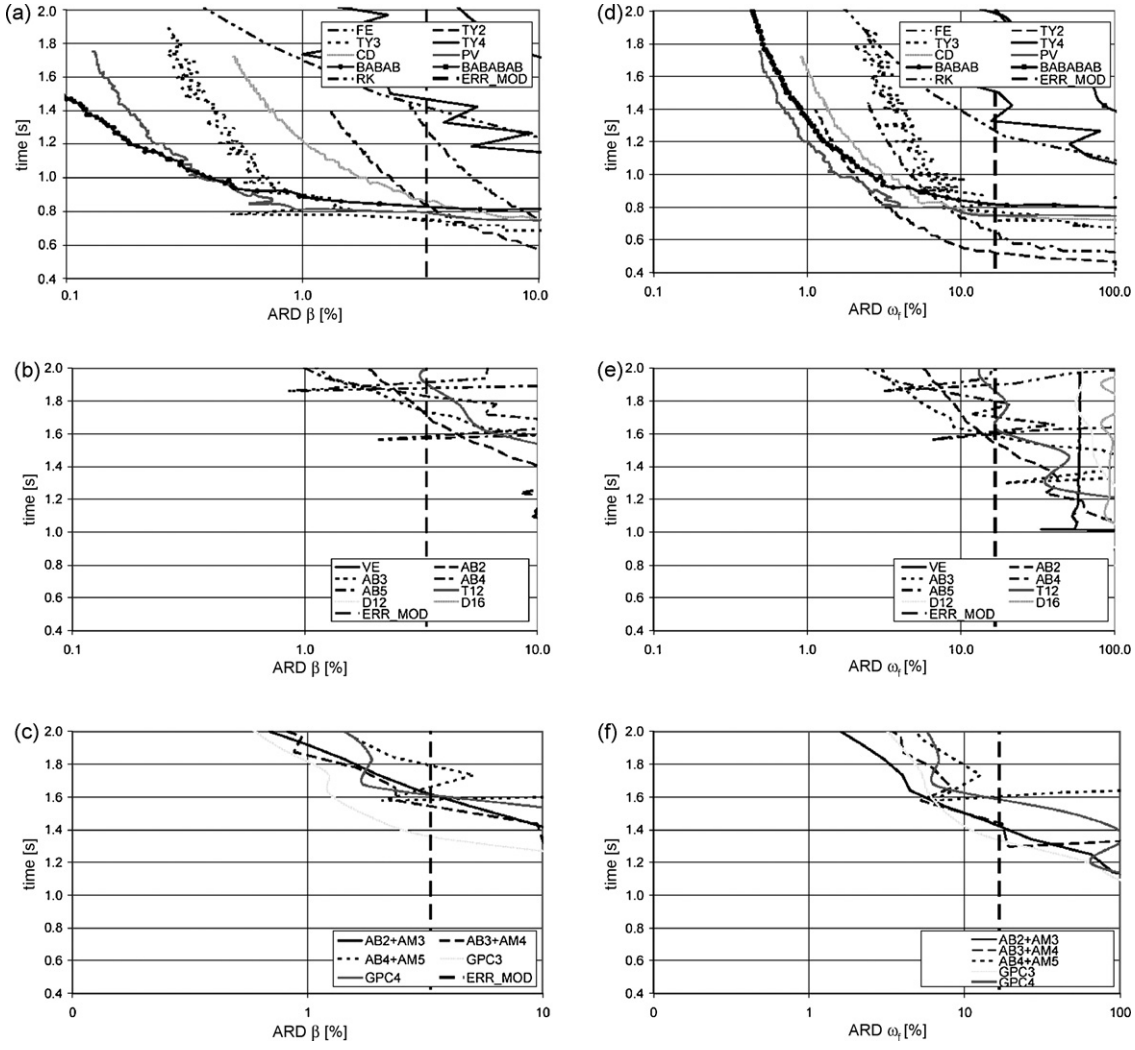

Fig. 9. CPU requirement over the average deviation of the rebound angle β (a–c) and the final rotational speed ω_f (d–f) between the exact analytical and a numerical solution with varying integration steps for the impact problem by Gorham and Kharaz (2000) for a set of integration schemes.

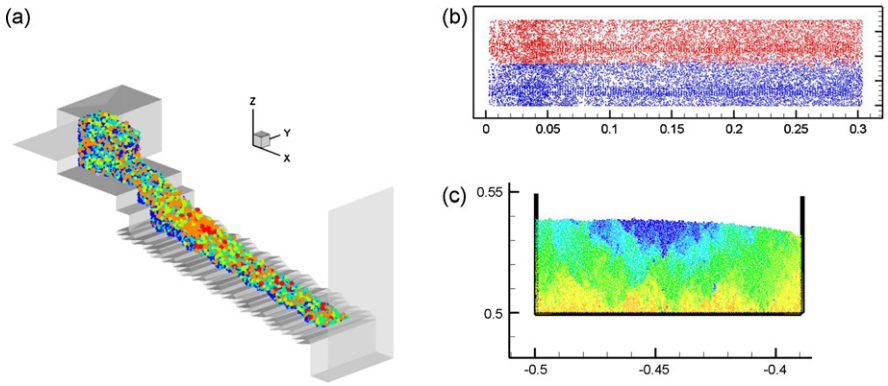

Fig. 10. Simulation examples: a three-dimensional forward acting grate (a), three-dimensional mixing on a vibrating conveyor (b) and 2D shear band formation (c).

of 3%. In general, simple algorithms appear to be more efficient than more complex algorithms.

Results on the efficiency for modeling the rebound angle β and the final rotational speed ω_f are presented in Fig. 9. Again, the model error of 3.52% for the rebound angle and 12% for the final rotational speed are illustrated as dotted lines. From the point of computational efficiency, the more simple algorithms seem to dominate at least for the studied range of intended accuracies. If an accuracy of at least twice the size of the model error is intended the position Verlet (PV), or the Taylor expansion of

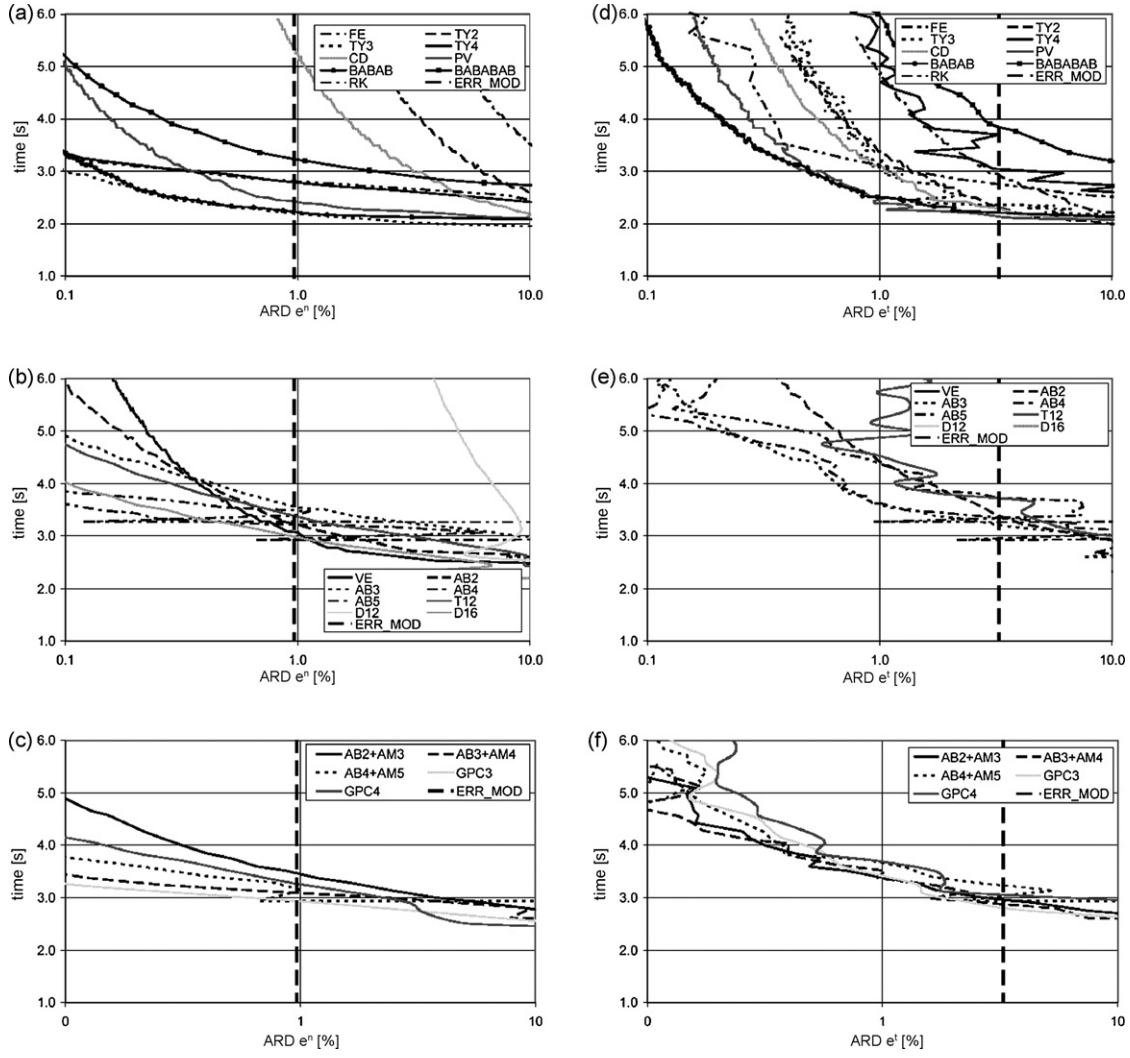

Fig. 11. CPU requirement including contact detection over the average deviation of the normal coefficient of restitution e^n (a–c) and the tangential coefficient of restitution e^t (d–f) between the exact analytical and a numerical solution with varying integration steps for the impact problem by Gorham and Kharaz (2000) for a set of integration schemes.

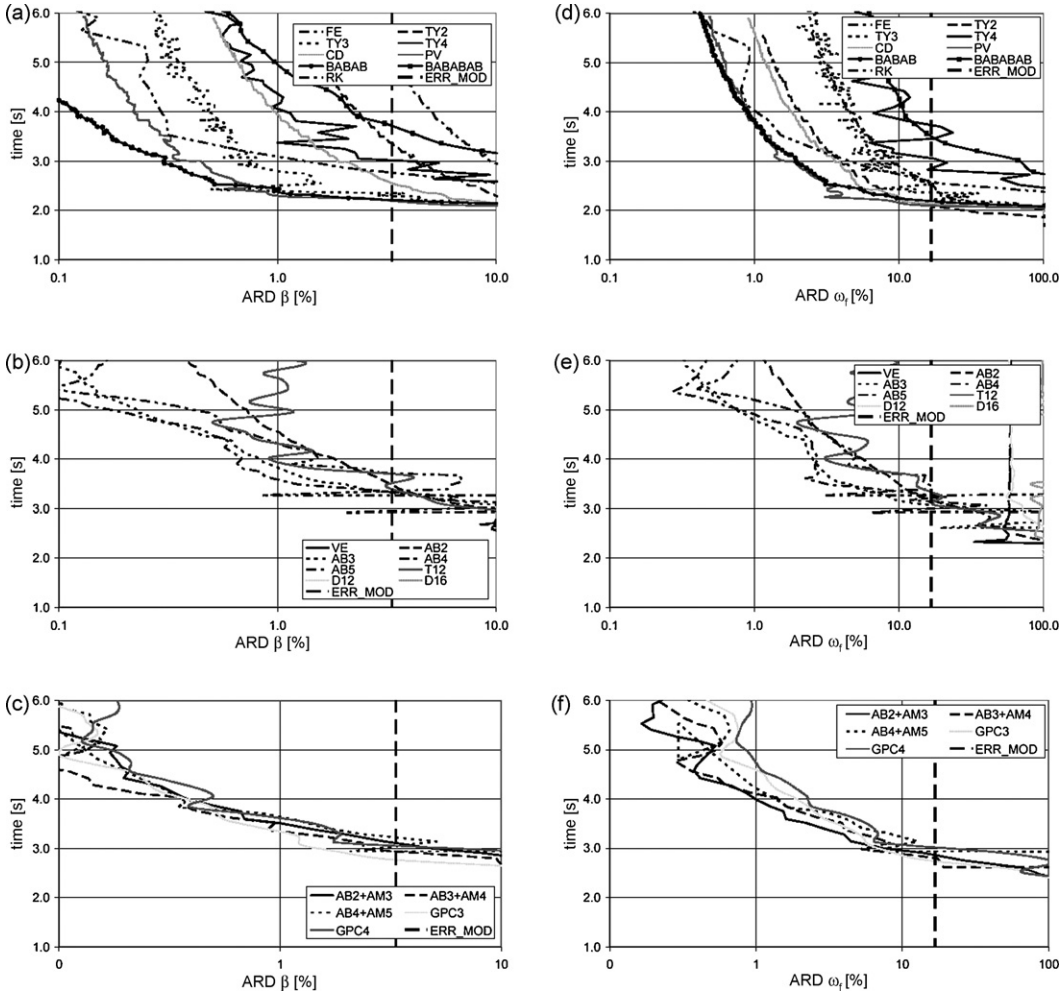

Fig. 12. CPU requirement including contact detection over the average deviation of the rebound angle β (a–c) and the final rotational speed ω_f (d–f) between the exact analytical and a numerical solution with varying integration steps for the impact problem by Gorham and Kharaz (2000) for a set of integration schemes.

third order achieves this goal with a step number of around 25 for the rebound angle. The error introduced through the fixed grid is in the range of 3%. For the final rotational speed the Taylor expansion of second order turns out to be a good choice, whereas here integration step numbers of 22 are necessary, resulting in a grid error of 9%.

The efficiency of an integration scheme cannot only be evaluated based on the accuracy and the computing time necessary for the integration itself. In a realistic discrete element Simulation contact detection, force calculation, and other auxiliary tasks take up most of the time. Measurements within different simulation examples as shown in Fig. 10 have revealed that the integration itself accounts only for 10–40% of the whole computational load depending on the simulation analyzed in case that a simple second order Taylor series expansion integrator is used. Cases studied include a three-dimensional forward acting grate (a), three-dimensional mixing on a vibrating conveyor (b), and two-dimensional shear band formation (c).

The time necessary for contact detection and force calculation depends on the density of the granular system. If the density of a granular system is increased, the computing time necessary for contact detection and force calculation inclines more strongly than the computing time necessary for the integration of the equations of motion. The portion of computing time necessary for integrating the equations of motion is larger for three-dimensional in contrast to two-dimensional simulations. The fraction of computing time necessary for the integration is smallest for the forward acting grate, followed by the three-dimensional mixing on the conveyor and largest for the simulation of shear band formation. For a more detailed discussion on this topic, especially the influence of programming languages and different DEM-techniques, it is referred to Balevicius, Dziugys, Kacianauskas, Maknickas, and Vislavicius (2006).

In Fig. 11 the effect of the additional computing time necessary for contact detection and force calculation is considered in the computational demand over accuracy plots. Results are based on an average ratio of 25% determined and measured as the computational demand for the integration of the equations of motion from the applications shown in Fig. 10. It is obvious that such a ratio directly favors more complex algorithms, due to the fact that their computational demand is of secondary importance in comparison to the more expensive contact detection and force calculation. For the normal coefficient of restitution the Taylor

expansion of third order TY3 is still the most efficient algorithm, however, it is directly followed by the improved Verlet scheme (BABAB), the position Verlet (PV) and the Runge-Kutta method. The differences in efficiency between one-step methods and predictor–corrector schemes vanish. A similar situation turns out for the coefficient of tangential restitution. Most favorable algorithms are the position Verlet (PV) directly followed by the Verlet (BABAB) scheme (Fig. 12).

Results for the rebound angle β and the final rotational speed ω_f confirm observations made for the coefficients of restitution. In cases where most computing time is spend on other tasks than the integration itself medium complex algorithms turn out as most superior. Complex algorithms cannot gain enough advantage due to the discontinuity of the differential equations operating on. Algorithms used best are the position Verlet (PV), or the improved Verlet (BABAB) scheme.

5. Conclusions

By modeling a particle–wall collision, which is a typical problem arising within granular dynamics, different mostly explicit numerical integration schemes have been tested for their performance within the discrete element method. Although only individual particles from one impact experiment (Gorham & Kharaz, 2000) have been considered in this study the results obtained are of general validity for any kind of discrete element simulation. First by addressing the integration accuracy on the basis of the step number n, which is the number of intervals the duration of a collision is divided in, it becomes independent of geometric size and the mass of the impacting particle. Secondly, the discrete element method is a physical, discrete method, therefore the modeling accuracy on the single grain level directly influences the accuracy on larger scales.

As models simple linear spring damper approaches have been used in normal and tangential direction. This allows for an analytical solution of the set of ordinary differential equations describing the contact. Algorithms have been analyzed regarding to their accuracy and their demand for computing time with integration step numbers varying in ranges as suggested in literature.

The accuracy of the methods was benchmarked for a number of collision properties. Big differences in accuracy were detected for collision properties related to the normal and tangential direction. Whereas in the first case the ordinary differential equation is continuous it is only continuous in an interval over time for the latter. In case of tangential collision properties, this results in an oscillating behavior of the accuracy over the integration step number for some schemes. Regarding the accuracy, the influence of a fixed time grid on collision properties was analyzed, too. Calculations for the worst case revealed that step numbers larger than 25 are already expedient regardless of the integration scheme applied. The only exception is the normal coefficient of restitution. Here the time grid error exceeds the integration error strongly.

Combining accuracy and computing time results in identification of the most efficient algorithms. However, it is not sufficient just to consider the computational time for the integration itself but also the time needed for force calculation and contact detection. These influences are highly dependent on the kind of simulation performed and have to be considered on a case-by-case basis. The higher the additional computational cost the more complex integration schemes are feasible. In general collision properties can be resolved with a high enough accuracy in case of algorithms presented here if a step size number larger than 20 is selected. Most favorable algorithms seem to be the Taylor expansion of order two and three or in cases with a higher computational cost the improved Verlet scheme (BABAB). Especially for large-scale simulations the integration method and the number of steps used has a tremendous impact on the overall performance of the simulation.

Acknowledgements

The authors thank S. Strüken for assisting them with parts of this analysis. The support by the Studienstiftung des Deutschen Volkes is gratefully acknowledged.

References

Allen, M. P., & Tildesley, D. J. (1989). *Computer simulations of liquids*. Oxford: Clarendon Press.

Arratia, P. E., Duong, N. H., Muzzio, F. J., Godbole, P., & Reynolds, S. (2006). A study of the mixing and segregation mechanisms in the Bohle Tote blender via DEM simulations. *Powder Technology*, *164*(1), 50–57.

Balevicius, R., Dziugys, A., Kacianauskas, R., Maknickas, A., & Vislavicius, K. (2006). Investigation of performance of programming approaches and languages used for numerical simulation of granular material by the discrete element method. *Computer Physics Communications*, *175*(6), 404–415.

Balevicius, R., Kacianauskas, R., Mroz, Z., & Sielamowicz, I. (2006). Discrete element method applied to multiobjective optimization of discharge flow parameters in hoppers. *Structural and Multidisciplinary Optimization*, *31*(3), 163–175.

Bertrand, F., Leclaire, L. A., & Levecque, G. (2005). DEM-based models for the mixing of granular materials. *Chemical Engineering Science*, *60*(8–9), 2517–2531.

Butcher, J. C. (1987). *The numerical analysis of ordinary differential equations: Runge-Kutta and general linear methods*. New York, NY, USA: Wiley-Interscience.

Chiesa, M., Melheim, J. A., Pedersen, A., Ingebrigtsen, S., & Berg, G. (2005). Forces acting on water droplets falling in oil under the influence of an electric field: Numerical predictions versus experimental observations. *European Journal of Mechanics B: Fluids*, *24*(6), 717–732.

Corliss, G., & Chang, Y. F. (1982). Solving ordinary differential-equations using Taylor-series. *ACM Transactions on Mathematical Software*, *8*(2), 114–144.

Cundall, P. A., & Strack, O. D. L. (1979). A discrete numerical model for granular assemblies. *Geotechnique*, *29*, 47–65.

Di Maio, F. P., & Di Renzo, A. (2004). Analytical solution for the problem of frictional-elastic collisions of spherical particles using the linear model. *Chemical Engineering Science*, *59*(16), 3461–3475.

Dintwa, E., van Zeebroeck, M., Tijskens, E., & Ramon, H. (2004). Torsional stiffness of viscoelastic spheres in contact. *The European Physical Journal B*, *39*, 77–85.

Di Renzo, A., & Di Maio, F. P. (2004). Comparison of contact-force models for the simulation of collisions in DEM-based granular flow codes. *Chemical Engineering Science*, *59*, 525–541.

Dury, C. M., & Ristow, G. H. (1997). Radial segregation in a two-dimensional rotating drum. *Journal de Physique I*, *7*(5), 737–745.

Engeln-Mullges, G., & Uhlig, F. (1996). *Numerical algorithms with Fortran*. Springer.

Forest, E., & Ruth, R. D. (1990). Fourth-order symplectic integration. *Physica D*, *43*, 105–117.

Fraige, F. Y., & Langston, P. A. (2004). Integration schemes and damping algorithms in distinct element models. *Advanced Powder Technology*, *15*(2), 227–245.

Gorham, D. A., & Kharaz, A. H. (2000). The measurement of particle rebound characteristics. *Powder Technology*, *112*(3), 193–202.

Hertz, H. (1882). Ueber die Berührung fester elastischer Koerper. *Journal für die reine und angewandte Mathematik*, *92*, 156–171.

Khakimov, Z. M. (2002). New integrator for molecular dynamics simulations. *Computer Physics Communications*, *147*, 733–736.

Kruggel-Emden, H., Simsek, E., Rickelt, S., Wirtz, S., & Scherer, V. (2007). Review and extension of normal force models for the discrete element method. *Powder Technology*, *171*(3), 157–173.

Kruggel-Emden, H., Simsek, E., Wirtz, S., & Scherer, V. (2006). Modeling of granular flow and combined heat transfer in hoppers by the discrete element method (DEM). *Journal of Pressure Vessel Technology*, *128*(3), 439–444.

Kruggel-Emden, H., Simsek, E., Wirtz, S., & Scherer, V. (2007). A comparative numerical study of particle mixing on different grate designs through the discrete element method. *Journal of Pressure Vessel Technology*, *129*(4), 529–600.

Kruggel-Emden, H., Wirtz, S., & Scherer, V. (in press). A study on tangential force laws applicable to the discrete element method (DEM) for materials with viscoelastic or plastic behavior. *Chemical Engineering Science*.

Kruggel-Emden, H., Wirtz, S., & Scherer, V. (2007). An analytical solution of different configurations of the linear viscoelastic normal and frictional-elastic tangential contact model. *Chemical Engineering Science*, *62*(23), 6914–6926.

Kwapinska, M., Saage, G., & Tsotsas, E. (2006). Mixing of particles in rotary drums: A comparison of discrete element simulations with experimental results and penetration models for thermal processes. *Powder Technology*, *161*(1), 69–78.

Langston, P. A., Tüzün, U., & Heyes, D. M. (1994). Continuous potential discrete particle simulations of stress and velocity fields in hoppers: Transition from fluid to granular flow. *Chemical Engineering Science*, *49*(8), 1259–1275.

Limtrakul, S., Boonsrirat, A., & Vatanatham, T. (2004). DEM modeling and simulation of a catalytic gas–solid fluidized bed reactor: A spouted bed as a case study. *Chemical Engineering Science*, *59*, 5225–5231.

Maw, N., Barber, J. R., & Fawcett, J. N. (1976). The oblique impact of elastic spheres. *Wear*, *38*, 101–114.

Melheim, J. A. (2005). Cluster integration method in Lagrangian particle dynamics. *Computer Physics Communications*, *171*(3), 155–161.

Moon, S. J., Kevrekidis, I. G., & Sundaresan, S. (2006). Particle simulation of vibrated gas-fluidized beds of cohesive fine powders. *Industrial & Engineering Chemistry Research*, *45*(21), 6966–6977.

Munjiza, A., & Andrews, K. R. F. (1998). NBS contact detection algorithm for bodies of similar size. *International Journal for Numerical Methods in Engineering*, *43*(1), 131–149.

Munjiza, A., Rougier, E., & John, N. W. M. (2006). MR linear contact detection algorithm. *International Journal for Numerical Methods in Engineering*, *66*(1), 46–71.

Omelyan, I. P., Mryglod, I. M., & Folk, R. (2002a). Optimized Verlet-like algorithms for molecular dynamics simulations. *Physical Review E*, *65*(5). Art. No. 056706 Part 2.

Omelyan, I. P., Mryglod, I. M., & Folk, R. (2002b). New optimized algorithms for molecular dynamics simulations. *Condensed Matter Physics*, *5*(31), 369–390. No. 3.

O'Sullivan, C., & Bray, J. D. (2004). Selecting a suitable time step for discrete element simulations that use the central difference time integration scheme. *Engineering Computations*, *21*(2–4), 278–303.

Ovesen, J. H., Petersen, H. G., & Perram, J. W. (1996). Comparison of two methods for solving linear equations occurring in molecular dynamics applications. *Computer Physics Communications*, *94*(1), 1–18.

Pandey, P., Song, Y. X., Kayihan, F., & Turton, R. (2006). Simulation of particle movement in a pan coating device using discrete element modeling and its comparison with video-imaging experiments. *Powder Technology*, *161*(2), 79–88.

Peters, B., Dziugys, A., Hunsinger, H., & Krebs, L. (2005). An approach to qualify the intensity of mixing on a forward acting grate. *Chemical Engineering Science*, *60*(6), 1649–1659.

Pöschel, T., & Schwager, T. (2005). *Computational granular dynamics—Models and algorithms*. Springer.

Rougier, E., Munjiza, A., & John, N. W. A. (2004). Numerical comparison of some explicit time integration schemes used in DEM, FEM/DEM and molecular dynamics. *International Journal for Numerical Methods in Engineering*, *61*(6), 856–879.

Sadd, M. H., Tai, Q. M., & Shukla, A. (1993). Contact law effects on wave-propagation in particulate materials using distinct element modeling. *International Journal of Non-Linear Mechanics*, *28*(2), 251–265.

Schäfer, J., Dippel, S., & Wolf, D. E. (1996). Force schemes in simulations of granular materials. *Journal de Physique I*, *6*(1), 5–20.

Schinner, A. (1999). Fast algorithms for the simulations of polygonal particles. *Granular Matter*, *2*(1), 35–43.

Shampine, L. F. (1994). *Numerical solution of ordinary differential equations*. New York: Chapman & Hall.

Stevens, A. B., & Hrenya, C. M. (2005). Comparison of soft-sphere models to measurements of collision properties during normal impacts. *Powder Technology*, *154*(2–3), 99–109.

Sundaram, S., & Collins, L. R. (1996). Numerical considerations in simulating a turbulent suspension of finite-volume particles. *Journal of Computational Physics*, *124*(2), 337–350.

Taguchi, Y. H. (1992a). New origin of a convective motion—Elastically induced convection in granular-materials. *Physical Review Letters*, *69*(9), 1367–1370.

Taguchi, Y. H. (1992b). Powder turbulence—Direct onset of turbulent-flow. *Journal de Physique II*, *2*(12), 2103–2114.

Takeuchi, S., Wang, S., & Rhodes, M. (2004). Discrete element simulation of a flat-bottomed spouted bed in the 3D cylindrical coordinate system. *Chemical Engineering Science*, *59*(17), 3495–3504.

Tatemoto, Y., Mawatari, Y., & Noda, K. (2005). Numerical simulation of cohesive particle motion in vibrated fluidized bed. *Chemical Engineering Science*, *60*(18), 5010–5021.

Thompson, P. A., & Grest, G. S. (1991). Granular flow—Friction and the dilatancy transition. *Physical Review Letters*, *67*(13), 1751–1754.

Tsuji, Y., Tanaka, T., & Ishida, T. (1992). Lagrangian numerical simulation of plug flow of cohesionless particles in a horizontal pipe. *Powder Technology*, *71*, 239–250.

Tuckerman, M., Berne, B. J., & Martyna, G. J. (1993). Reply to comment on: Reversible multiple time scale molecular dynamics. *Journal of Chemical Physics*, *99*, 2278–2279.

Van Puyvelde, D. R. (2006). Comparison of discrete elemental modelling to experimental data regarding mixing of solids in the transverse direction of a rotating kiln. *Chemical Engineering Science*, *61*(13), 4462–4465.

Verlet, L. (1967). Computer experiments on classical fluids. I. Thermodynamical properties of Lennard–Jones molecules. *Physical Review*, *159*(1), 98–103.

Yang, R. Y., Zou, R. P., & Yu, A. B. (2003). Microdynamic analysis of particle flow in a horizontal rotating drum. *Powder Technology*, *130*(1–3), 138–146. Sp. Iss. SI.

Zhang, D., & Whiten, W. J. (1996). The calculation of contact forces between particles using spring and damping models. *Powder Technology*, *88*, 59–64.

Zhang, D., & Whiten, W. J. (1998). An efficient calculation method for particle motion in discrete element simulations. *Powder Technology*, *98*(3), 223–230.

Zhang, D., & Whiten, W. J. (2001). Step size control for efficient discrete element simulation. *Minerals Engineering*, *14*(10), 1341–1346.

Zhong, W. Q., Xiong, Y. Q., Yuan, Z. L., & Zhang, M. Y. (2006). DEM simulation of gas–solid flow behaviors in spout-fluid bed. *Chemical Engineering Science*, *61*(5), 1571–1584.

Zhu, H. P., & Yu, A. B. (2004). Steady-state granular flow in a three-dimensional cylindrical hopper with flat bottom: Microscopic analysis. *Journal of Physics D: Applied Physics*, *37*(10), 1497–1508.

Zhu, H. P., & Yu, A. B. (2005). Steady-state granular flow in a 3D cylindrical hopper with flat bottom: Macroscopic analysis. *Granular Matter*, *7*(2–3), 97–107.